Journal of Applied Polymer Science

Morphology and Crystallization Behavior of Nylon 6-Clay/Neat Nylon 6 Bicomponent Nanocomposite Fibers

Shahin Kazemi,[1] Mohammad Reza Mohaddes Mojtahedi,[1] Wataru Takarada,[2] Takeshi Kikutani[2]

[1]Department of Textile Engineering, Amirkabir University of Technology, Tehran, Iran

[2]Department of Organic and Polymeric Materials, Graduate School of Science and Engineering, Tokyo Institute of Technology, Tokyo 152-8552, Japan

Correspondence to: M. R. M. Mojtahedi (E-mail; mojtahed@aut.ac.ir)

ABSTRACT: Nylon 6-clay hybrid/neat nylon 6, sheath/core bicomponent nanocomposite fibers containing 4 wt % of clay in sheath section, were melt spun at different take-up speeds. Their molecular orientation and crystalline structure were compared to those of neat nylon 6 fibers. Moreover, the morphology of the bicomponent fibers and dispersion of clay within the fibers were analyzed using scanning electron microscopy and transmission electron microscopy (TEM), respectively. Birefringence measurements showed that the orientation development in sheath part was reasonably high while core part showed negligibly low birefringence. Results of differential scanning calorimetry showed that crystallinity of bicomponent fibers was lower than that of neat nylon 6 fibers. The peaks of γ-crystalline form were observed in the wide-angle X-ray diffraction of bicomponent and neat nylon 6 fibers in the whole take-up speed, while α-crystalline form started to appear at high speeds in bicomponent fibers. TEM micrographs revealed that the clay platelets were individually and evenly dispersed in the nylon 6 matrix. The neat nylon 6 fibers had a smooth surface while striped pattern was observed on the surface of bicomponent fibers containing clay. This was speculated to be due to thermal shrinkage of the core part after solidification of the sheath part in the spin-line. © 2013 Wiley Periodicals, Inc. J. Appl. Polym. Sci. **2014**, *131*, 39996.

KEYWORDS: bicomponent fibers; nylon 6-clay hybrid; morphology; crystallization

Received 10 July 2013; accepted 23 September 2013

DOI: 10.1002/app.39996

INTRODUCTION

In recent years, polymer-based composite hybrid materials have attracted significant interests and numerous studies have been devoted to this subject. Modification of polymer by adding nanofiller becomes a practical strategy to improve the parent polymer material properties. Among the nanofillers, nano layered silicate (clay) has received much attention and wide range of thermoplastics have been reinforced with this material.[1–8]

Polymer/layered silicate nanocomposites exhibit outstanding improvement in material properties as compared to conventional composites. These enhancements in properties include reinforced mechanical properties, better thermal stability, reduced gas permeability, and improved fire retardancy.[9–12]

Nylon 6 is a semicrystalline polymer possessing outstanding physical and mechanical properties. Therefore, many researchers have studied the influence of nanoclay additive on the processing behavior as well as structure and morphology of nylon 6-clay hybrid (NCH). Nevertheless, studies on the NYH fiber are limited. Giza et al. compared the structures of neat nylon 6 and NYH fibers prepared at different take-up speeds and draw ratios.[13,14] The thermal properties, orientation and structural changes of clay filled nylon 6 fibers have also been investigated as a function of melt temperature by Ergungor et al.[15] The effect of annealing on structure and properties of nylon 6-clay (NYC) fibers has been studied by Yoon et al.[16] Ibanes et al. described the microstructure changes and deformation mechanisms in spun and drawn nylon 6 fibers containing clay.[17,18] Recently, Joshi et al. prepared filaments and their cord of NYC nanocomposite with two different clays.[19] Steinmann et al. determined the influence of nano-phyllosilicates on the drawability of nylon 6 filaments.[20] The drawing behavior and ultimate tenacity of the nylon 6/NYC composite fibers prepared by varying NYC contents and drawing temperatures were systematically investigated by Yeh et al.[21].

As per our knowledge, no literature concerning the effect of clay in bicomponent NCH/nylon 6 fibers is available. In this work, we fabricated NCH/nylon 6 bicomponent fibers via melt

Table I. Spinning Conditions for Neat Nylon 6 and BiCo Fibers

	Neat nylon 6	BiCo
First extruder temperature profile (°C)	240, 250, 260, 260	240, 250, 260, 260
Second extruder temperature profile (°C)	Not used	240, 260, 260
Spinning head temperature (°C)	260	260
Extruder *L/D*	25	25
Mass flow rate (g/min)	5	2.5 for each part
Nozzle diameter (mm)	1	1
Nozzle hole *L/D*	3	3
Take-up speed (m/min)	25–5000	25–5000

spinning process at different take-up speeds and the structural changes of the bicomponent fibers were investigated.

EXPERIMENTAL

Materials

The materials used in this study, neat nylon 6 and NCH masterbatch containing 4 wt % clay, were provided by Nanopolymer Composites Corporation, Taiwan. The NCH masterbatch under commercial name of NE2640 was reported to be produced via in situ polymerization with a montmorillonite (Cloisite 30B from Southern Clay Products, Inc.) modified by methyl, tallow, bis-2-hydroxyethyl quaternary ammonium chloride. The nylon 6 chips with a commercial name of A2500 were used. The polymer had a relative viscosity of 2.5.

Melt Spinning of Filaments

The polymer chips were dried in a vacuum oven for at least 12 h at 110°C prior to spinning. Melt spinning was carried out using a spinning apparatus (Musashino Kikai Co., Ltd., Japan). Filaments were extruded from the spinneret through a single-hole nozzle with a diameter of 1 mm and were taken up by a high-speed winder located 330 cm below spinneret. No spin finish and external quench cabinet was used. The spinning conditions are summarized in Table I.

The bicomponent fiber was produced in sheath–core form in which the sheath and core parts were NCH and neat nylon 6, respectively. The details of sheath–core fiber production process were explained in the previous works.[22–25] The weight fraction of both parts was the same (50/50). Hereafter, this fiber is named BiCo.

Measurements

Birefringence of fibers was obtained using an interference microscope (Carl Zeiss Jena, Germany) according to procedure described in the previous work.[22] The average of the measurements for ten individual fibers is reported.

Differential scanning calorimetry (DSC) was carried out by using a Q100 (TA Instruments, USA) device with a heating–cooling–heating cycle at heating and cooling rate of 10 °C/min in the range of 0–250°C under nitrogen atmosphere. The sample weight was 5–6 mg. The crystallinity of sample was calculated according to the following formula:

$$X_C(\%) = \frac{\Delta H_f}{\Delta H_f^\circ} \times 100 \quad (1)$$

where X_C is crystallinity percentage, ΔH_f refers to the measured melting enthalpy and ΔH_f° is the enthalpy of fusion of completely crystalline nylon 6 ($\Delta H_f^\circ = 213$ J/g).[23]

Wide angle X-ray scattering measurement was performed in transmission mode using a two-dimensional CCD camera on a Rigaku diffractometer (Rigaku, Japan) operated at 45 kV and 60 mA. The incident X-ray beam was monochromatized using a monochrometer to obtain CuKα radiation.

Transmission electron microscopy (TEM) was carried out on H-7650 microscope (Hitachi, Japan) using an acceleration voltage of 120 kV. Observations were made for ultramicrotomic slices cut parallel or perpendicular to the longitudinal direction of the fibers. The morphology of the fiber surface was studied using a scanning electron microscopy (SEM; SM-200, Topcon, Singapore) operated at 15 kV.

RESULTS AND DISCUSSION

Birefringence

The dependence of fiber birefringence on take-up speed is plotted in Figure 1. As expected, birefringence of neat nylon 6 fiber increased monotonically with take-up speed up to 3000 m/min, and then showed a tendency of saturation. The development of

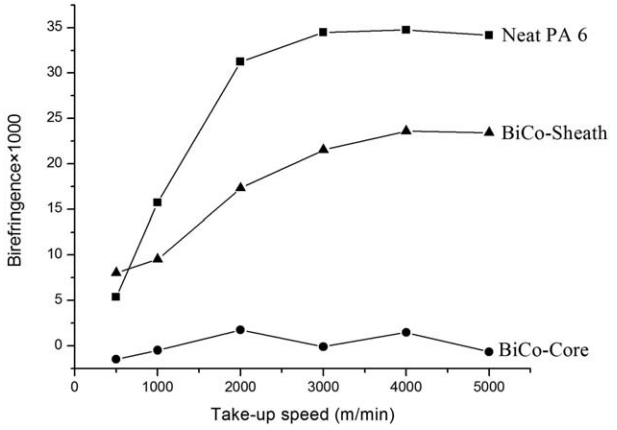

Figure 1. Birefringence values for neat nylon 6 fiber and sheath and core part of BiCo fibers prepared at different take-up speeds.

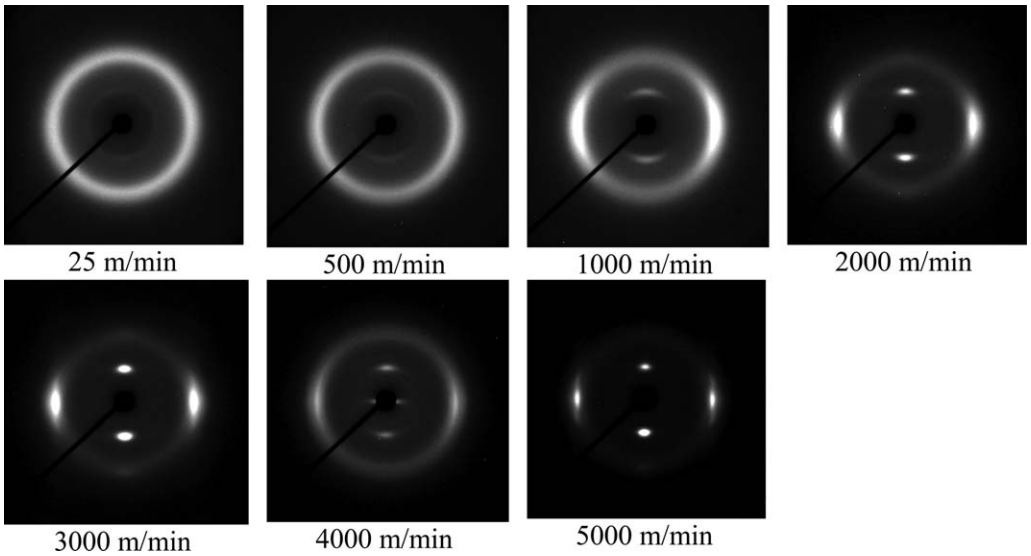

Figure 2. Wide-angle X-ray diffraction patterns of neat nylon 6 fibers prepared at different take-up speeds.

molecular orientation in fibers leads to an increase in birefringence. Similar behavior was observed in the sheath part of BiCo fibers; however the birefringence started to level off at a higher take-up speed of around 4000 m/min. Moreover, at take-up speed of 500 m/min, birefringence of the sheath part of BiCo fiber was higher than that of the neat nylon 6 fiber. Above 1000 m/min, birefringence of the neat nylon 6 fiber exceeded that of the sheath part of BiCo fiber. In both samples, the significant increase was observed at the take-up speed from 1000 to 2000 m/min.

On the other hand, the core part of BiCo fibers showed negligibly small birefringence. This result means that no orientation took place in this part. If the mechanism of orientation-induced crystallization in the melt spinning process is considered, the negligibly small birefringence in nylon 6 in BiCo suggests that the solidification/crystallization of the sheath part (NCH) occurred firstly in the spin-line, before the crystallization of the neat nylon 6. In this case, there can be even a progress of orientation relaxation in the neat nylon 6 during the cooling of the spin-line from the crystallization temperature of NCH to the glass transition temperature of nylon 6.[25]

One can speculate that higher viscosity in the sheath part compared to the core part is the possible reason for the behavior of birefringence development in the sheath and core parts. In this case, however, it is not possible to explain why the sheath part of BiCo has lower birefringence than the neat nylon 6. If viscosity of NCH is higher than that of neat nylon 6, and if both polymers have similar stress-optical coefficient, birefringence of NCH component in the BiCo fiber should be higher than that of neat nylon 6 of single component fiber.

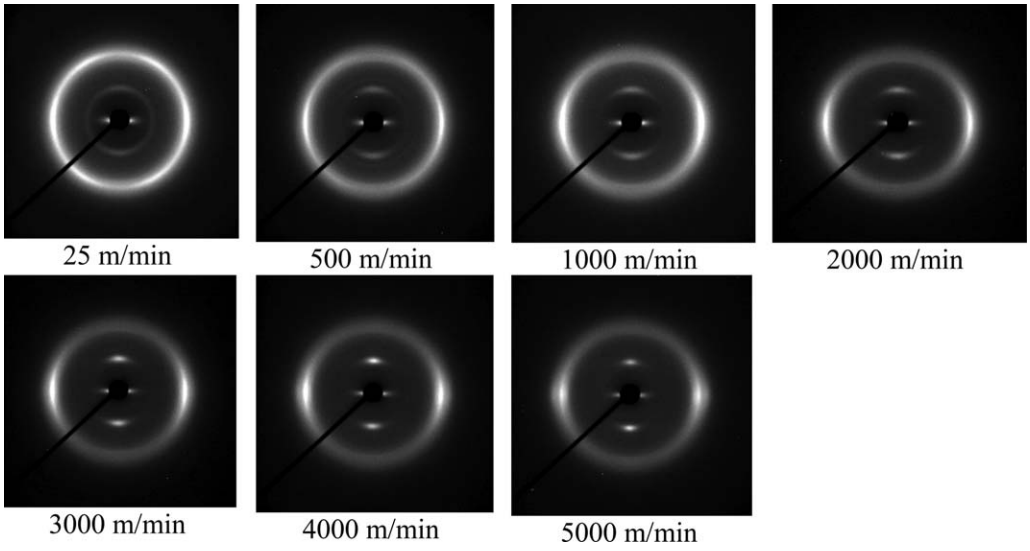

Figure 3. Wide-angle X-ray diffraction patterns of BiCo fibers prepared at different take-up speeds.

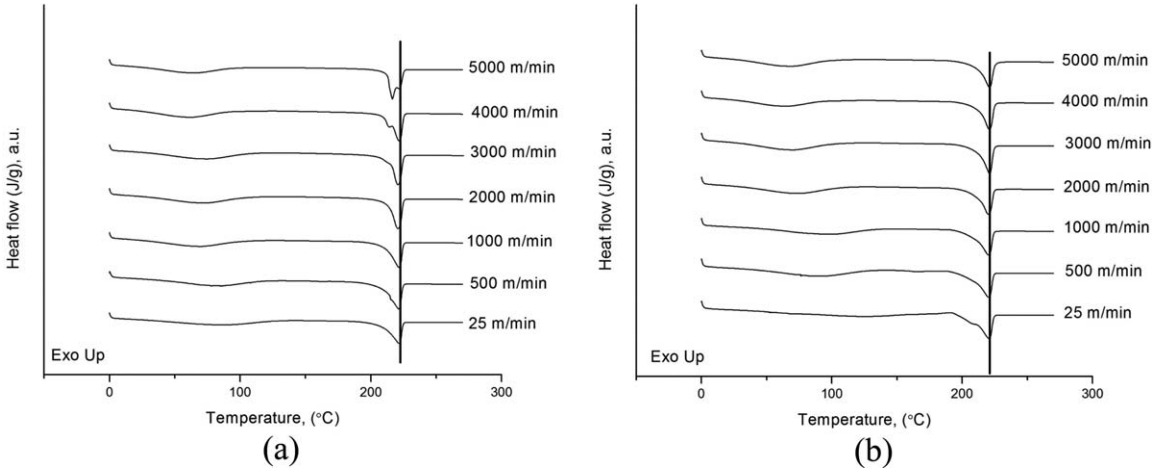

Figure 4. DSC thermograms of (a) neat nylon 6 and (b) BiCo fibers.

Accordingly, in the following discussion we need to discuss the mechanism of structure formation in BiCo fiber including the condition that NCH has lower viscosity than neat nylon 6. As reported in our previous research, thinning behavior in the spin-line of NYC proceeds more steeply in comparison with that of neat nylon 6 (see Figure 7 in Ref. 13). Solidification point tends to shift to upstream with the increase of take-up speed, while solidification point of NYC was always closer to the spinneret than neat nylon 6 at a certain take-up speed.[13] These results basically suggested that the variation of viscosity with temperature is more significant in NYC. In other words, viscosity of NCH has higher activation energy than that of neat nylon 6. In addition, the possibility of crystallization of NCH under elongational flow appears to be higher than the neat nylon 6.

Through the researches on bicomponent spinning of various combination of polymers, we have been discussing that in bicomponent spinning, structure formation of the component with higher activation energy (or higher T_g) would be enhanced while that of the polymer with lower activation energy would be suppressed.[22,24,25] The same scheme is applicable for the bicomponent spinning of NCH/nylon 6 in that structure formation of NYC is enhanced while that of nylon 6 is suppressed in comparison with the structure development in the single component melt spinning of individual component. It is important to note that this tendency is not affected by the absolute viscosity of each component.

Wide-Angle X-Ray Diffraction (WAXD)

WAXD patterns of neat nylon 6 and BiCo fibers prepared at different take-up speeds are presented in Figures 2 and 3, respectively. The WAXD patterns showed evident qualitative differences in crystallinity and crystalline orientation. Both neat nylon 6 and BiCo fibers spun at take-up speed of 25 m/min showed 2D pattern of circular symmetry. The crystalline orientation increased naturally with the increase of take-up speed. It should be noted that isotropic halo is much stronger in comparison with the intensity of crystalline reflections in BiCo fibers. This is another evidence that the orientation and crystallinity of the core part in these bicomponent fibers is low. The crystalline reflections in the WAXD patterns of neat nylon 6 fibers display characteristic features of γ-crystal structure as revealed by the $\gamma(200)$ and $\gamma(001)$ reflections on the equator and a crystalline peak of $\gamma(020)$ on the meridian. The WAXD patterns of BiCo fibers also showed similar peaks to those of neat nylon 6 fibers, while two additional crystalline peaks, which can be assigned to (200) and (002)/(202) reflections of α-crystalline form, started to appear on the equator at high speeds in bicomponent fibers.

It has been reported that, in high speed spinning of neat nylon 6, γ-form dominates the crystalline structure when orientation-induced crystallization starts with the increase of take-up speed; however α-form crystal starts to appear at extremely high speeds. In case of NCH, γ-form dominates the crystalline structure as in the case of neat nylon 6, whereas appearance of the

Table II. Thermal Properties of Melt-Spun Fibers Based on DSC Results

Sample	Take-up speed (m/min)	Heating cycle		
		T_{m1} (°C)	T_{m2} (°C)	Crystallinity (%)
PA 6	25	-	221.8	34.0
	500	-	221.3	35.9
	1000	-	221.6	36.6
	2000	-	220.6	37.6
	3000	212.6	220.6	38.1
	4000	214.1	221.5	38.4
	5000	216.3	221.9	38.5
BiCo	25	-	220.5	29.9
	500	-	220.3	32.5
	1000	-	220.1	31.4
	2000	-	220.2	32.3
	3000	-	221.0	33.0
	4000	-	220.7	33.4
	5000	-	220.9	34.0

T_{m1}: Lower melting temperature; T_{m2}: Higher melting temperature.

α-form crystals starts from lower take-up speed than neat nylon 6.[13] The experimental results shown in Figures 2 and 3 are in agreement with these findings.

Thermal Properties

Figure 4 shows the DSC thermograms of neat nylon 6 and BiCo fibers prepared at different take-up speeds. The melting peak temperature and crystallinity obtained from DSC measurements are summarized in Table II. As the take-up speed increases, crystallinity of the fibers increases gradually. Moreover, BiCo fibers showed lower crystallinity than neat nylon 6 fibers. Lower crystallinity of BiCo fibers is considered to be due to the lower crystallinity of neat nylon 6 in the core, which was speculated from the result of birefringence measurement. Considering small difference of crystallinity between neat nylon 6 and BiCo fibers, there is a possibility that NCH at sheath part in BiCo fiber has higher crystallinity than neat nylon 6 fiber at a given take-up speed.

As can be seen in Figure 4, neat nylon 6 fibers showed a shoulder of lower melting temperature at high speed region while BiCo fibers only showed single melting peak at all the take-up velocities. If it is assumed that the higher and lower melting peaks are related to α- and γ-crystalline forms, respectively, the α-crystalline form should predominate both in the neat nylon 6 and BiCo fibers at all take-up speeds. If discussion for the enhancement of the formation of α-form crystal in NCH at high take-up speeds is considered, we should observe

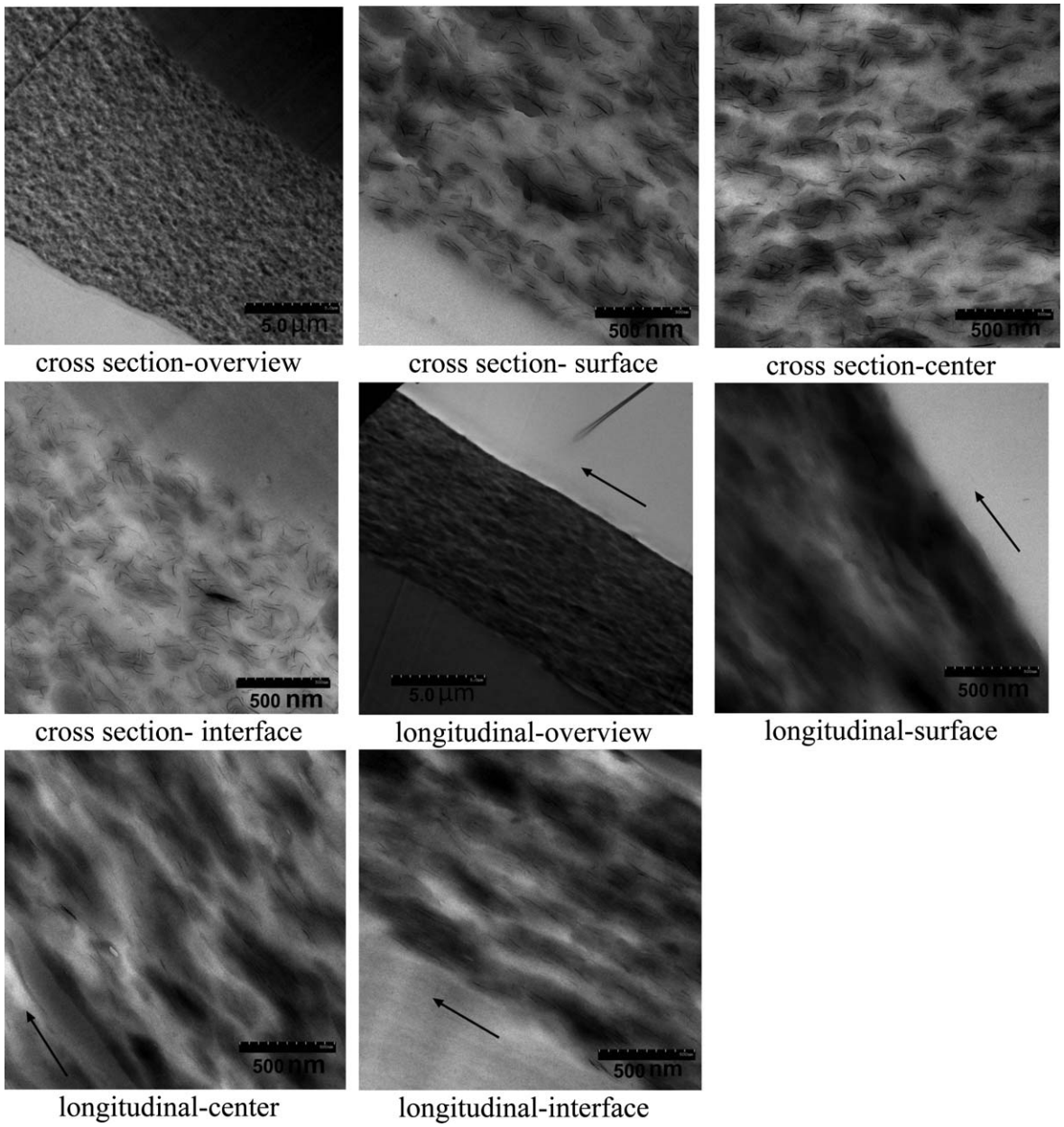

Figure 5. TEM micrographs for the cross- and longitudinal-sections of BiCo fibers at take-up speed of 500 m/min. In longitudinal images, the arrows show the fiber axis.

the lower and higher melting temperatures, while two melting peaks were observed only for the neat nylon 6 fibers prepared at high take-up speeds. Therefore, the experimental results suggest that the melting peak temperature does not necessarily represent the original structure in the fiber. In this context, there can be γ-crystals with different perfection, size, and stability in neat nylon 6 fibers. In the fibers spun at lower take-up speeds, the less grown, smaller crystallites of the γ-crystalline form were formed. Those crystals can be melted and re-crystallized to α-crystalline form with higher stability during DSC heating. On the other hand, γ-crystals with higher stability were formed in the fibers prepared at take-up speed of above 3000 m/min. Those crystals exhibit lower melting temperature of γ-form, while major part of the structure was converted to the α-crystalline form during DSC heating and exhibits higher melting temperature. In case of NYC fibers prepared at all the take-up speeds, it seems that crystalline structure can be converted to more ordered α-form structure easily during the heating process in DSC. This is considered to be an intrinsic characteristic of NCH. For more detailed discussion, we need modulated DSC analysis of this sample in the future.

Morphology

Transmission electron micrograph was used to investigate the microstructure and dispersion characteristics of NYC nanocomposites. TEM images were taken for the sliced sections cut perpendicular and parallel to the longitudinal direction of the fiber samples (cross-section and longitudinal-section) spun at low

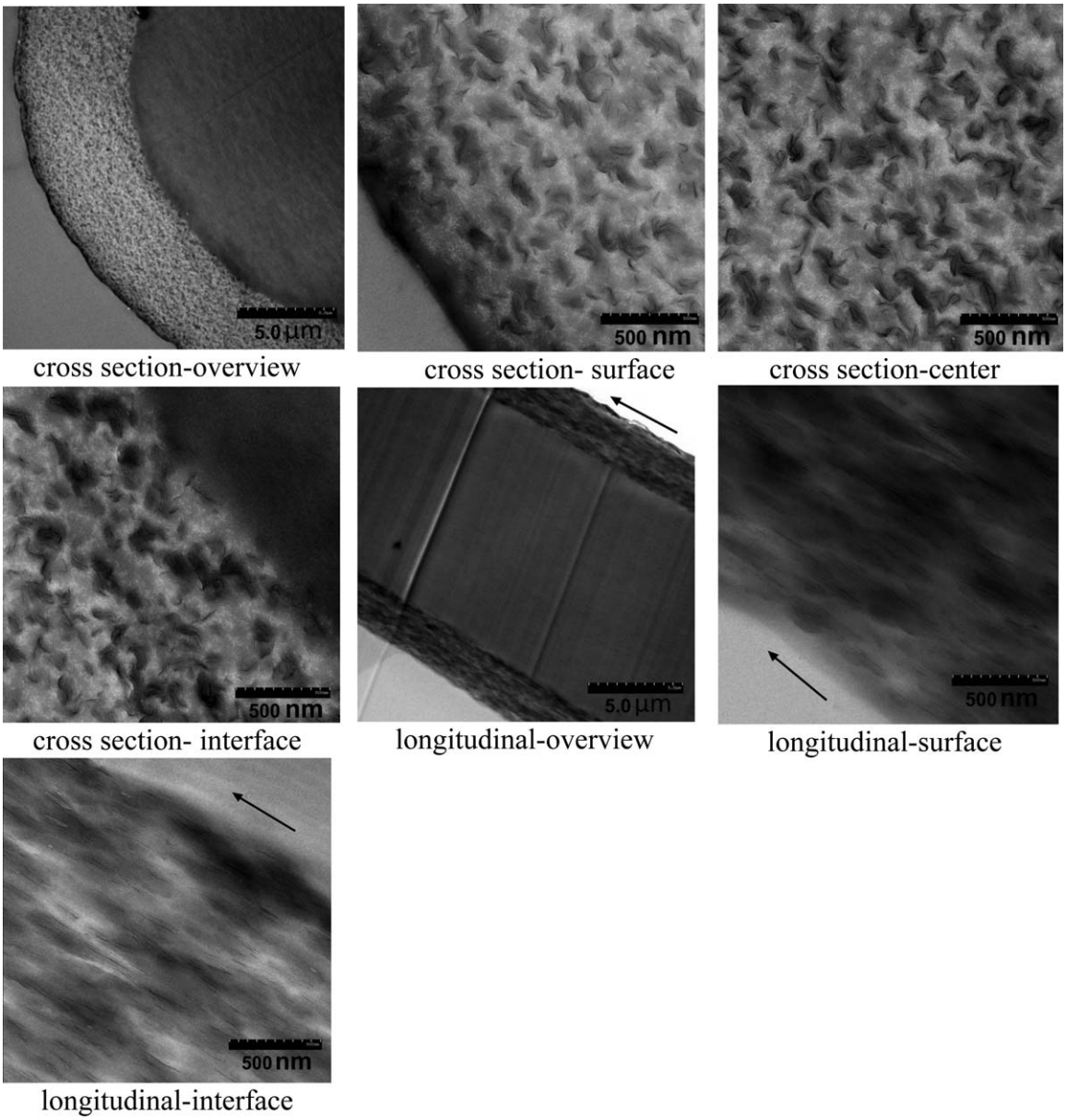

Figure 6. TEM micrographs for the cross- and longitudinal-sections of BiCo fibers at take-up speed of 5000 m/min. In longitudinal images, the arrows show the fiber axis.

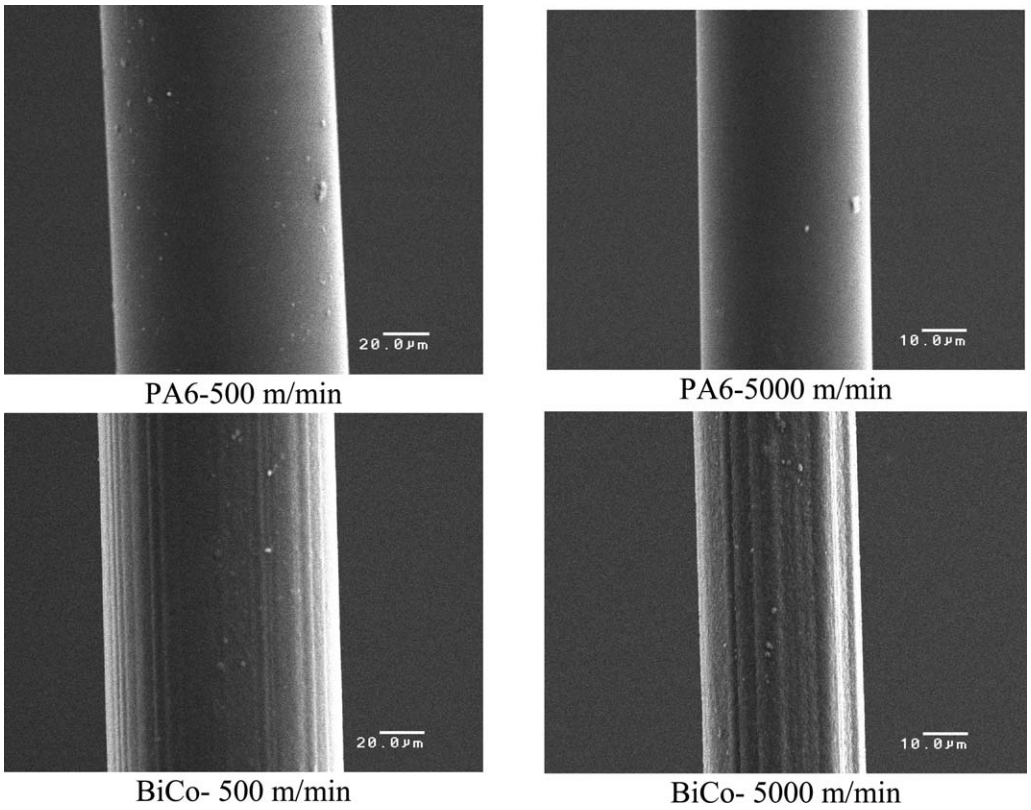

Figure 7. SEM micrographs of the nylon 6 and BiCo fibers prepared at two different take-up speeds.

and high take-up speeds. The results are shown in Figures 5 and 6, respectively. As can be seen, the state of dispersion of clay platelets is different in various parts of BiCo fibers including surface, center, and interface in the sheath part of bicomponent fibers. In both low and high take-up speeds, the clay dispersion at the center of sheath and near the interface of sheath–core is better than that at the surface of sheath. The center image for the longitudinal-section of the sample spun at 500 m/min showed that clay platelets are highly oriented even at low take-up speeds. An increase in take-up speed gives rise to better clay orientation. TEM pictures of longitudinal sections for the surface exhibited a few exfoliated platelets and big tactoids (Figure 5) while for the center, individual clay platelets were evenly dispersed in the polymeric matrix. A higher degree of intercalation was observed at higher take-up speeds probably due to strong shear and elongational stress and higher draw down ratio applied during the melt spinning process; however still large aggregates can be seen. The center part for the fiber spun at 5000 m/min was not observable by TEM due to low thickness of sheath layer.

Figure 7 shows SEM micrographs of neat nylon 6 and BiCo nanocomposite fibers. A smooth surface is observed in the SEM images of the neat nylon 6 fiber while the stripe is seen on the surface of BiCo fibers. The stripe may be related to the thermal shrinkage of the core part. As described in the Birefringence section, solidification (crystallization) of sheath part is speculated to occur at a temperature much higher than the T_g of nylon 6. Crystallized part supposed to have much lower thermal expansion coefficient than the polymer melt. Then the volume reduction of the core part with cooling is much more significant than that in the sheath, which leads to the development of stripe. These patterns are more pronounced in fibers spun at higher take-up speeds.

CONCLUSIONS

The results of current study illustrated that the sheath part had much higher orientation compared to core part in the BiCo fibers. The difference in crystallization rate of sheath and core parts in the BiCo fibers resulted in the remaining of the core part in the amorphous state. WAXD results showed that the γ-form crystals dominate the structure in both nylon 6 and BiCo fibers, while intensity of amorphous halo is stronger in BiCo fibers because of low crystallinity in the core part. On the other hand, addition of nanoclays promotes the formation of α-form crystals at extremely high speed region. The DSC thermograms suggested that there were γ-crystalline forms with different stabilities in neat nylon 6 fibers prepared at high-speeds, while NCH has an intrinsic characteristic of converting the crystalline structure from γ-form to more ordered α-form easily during the heating process in DSC. The DSC analysis also proved that BiCo fibers have lower crystallinity than neat nylon 6 fibers. In BiCo fibers, better dispersion and intercalation was obtained in the center of sheath and sheath–core interface. A higher take-up speed resulted in more intercalation. The striped pattern

appeared on the surface of BiCo fibers, while formation of the pattern was enhanced at higher take-up speeds.

REFERENCES

1. Mileva, D.; Monami, A.; Cavallo, D.; Alfonso, G. C.; Portale, G.; Androsch, R. *Macromol. Mater. Eng.* **2013**, *298*, 938.
2. Dong,Y.; Bhattacharyya, D. *J. Mater. Sci.* **2012**, *47*, 3900.
3. Fornes,T. D.; Paul, D. R. *Polymer* **2003**, *44*, 3945.
4. Paul, D. R.; Robeson, L. M. *Polymer* **2008**, *49*, 3187.
5. Okada, A.; Usuki, A. *Macromol. Mater. Eng.* **2006**, *291*, 1449.
6. LeBaron, P. C.; Wang, Z.; Pinnavaia, T. *J. Appl. Clay Sci.* **1999**, *15*, 11.
7. Hussain, F.; Hojjati, M.; Okamoto, M.; Gorga, R. E. *J. Compos. Mater.* **2006**, *40*, 1511.
8. Sinha Ray, S.; Okamoto, M. *Prog. Polym. Sci.* **2003**, *28*, 1539.
9. Alix, S.; Follain, N.; Tenn, N.; Alexandre, B.; Bourbigot, S.; Soulestin, J.; Marais, S. *J. Phys. Chem. C* **2012**, *116*, 4937.
10. Joshi, M.; Shaw, M.; Butola, B. S. *Fiber Polym.* **2004**, *5*, 59.
11. Choudalakis, G.; Gotsis, A. D. *Eur. Polym. J.* **2009**, *45*, 967.
12. Kiliaris, P.; Papaspyrides, C. D. *Prog. Polym. Sci.* **2010**, *35*, 902.
13. Giza, E.; Ito, H.; Kikutani, T.; Okui, N. *J. Macromol. Sci., Part B* **2000**, *39*, 545.
14. Giza, E.; Ito, H.; Kikutani, T.; Okui, N. *J. Polym. Eng.* **2000**, *20*, 403.
15. Ergungor, Z.; Cakmak, M.; Batur, C. *Macromol. Symp.* **2002**, *185*, 259.
16. Yoon, K.; Polk, M. B.; Min, B. G.; Schiraldi, D. A. *Polym. Int.* **2004**, *53*, 2072.
17. Ibanes, C.; David, L.; De Boissieu, M.; Séguéla, R.; Epicier T.; Robert, G. *J. Polym. Sci. Part B: Polym. Phys.* **2004**, *42*, 3876.
18. Ibanes, C.; David, L.; Seguela, R.; Rochas, C.; Robert, G. *J. Polym. Sci. Part B: Polym. Phys.* **2004**, *42*, 2633.
19. Joshi, M.; Biswas, D.; Sarvanan, A.; Purwar, R.; Mukhopadhaya, R. *J. Appl. Polym. Sci.* **2012**, *125*, E224.
20. Steinmann, W.; Walter, S.; Gries, T.; Seide, G.; Roth, G. *Text. Res. J.* **2012**, *82*, 1846.
21. Yeh, J.-T.; Wang, C.-K.; Liu, Z.-W.; Li, P.; Tsou, C.-H.; Lai, Y.-C.; Tsai, F.-C. *Polym. Eng. Sci.* **2012**, *52*, 1348.
22. Kikutani, T.; Radhakrishnan, J.; Arikawa, S.; Takaku, A.; Okui, N.; Jin, X.; Niwa, F.; Kudo, Y. *J. Appl. Polym. Sci.* **1996**, *62*, 1913.
23. Kojima, Y.; Usuki, A.; Kawasumi, M.; Okada, A.; Kurauchi, T.; Kamigaito, O.; Kaji, K. *J. Polym. Sci. Part B: Polym. Phys.* **1994**, *32*, 625.
24. Radhakrishnan, J.; Ito, H.; Kikutani, T.; Okui, N. *Polym. Eng. Sci.* **1999**, *39*, 89.
25. Radhakrishnan, J.; Ito, H.; Kikutani, T.; Okui, N. *Text. Res. J.* **1997**, *67*, 684.